

---

# Comparison of Complete Versus Fragmented Technetium-99m-Labeled Anti-CEA Monoclonal Antibodies for Immunoscintigraphy in Colorectal Cancer

Thomas M. Behr, Wolfgang S. Becker, Hans-J. Bair, Michael W. Klein, Christine M. Stühler, Klaus P. Cidlinsky, Christian W. Wittekind, Johannes R. Scheele and Friedrich G. Wolf

*Departments of Nuclear Medicine, Surgery, Radiology and Pathology, Friedrich-Alexander University of Erlangen-Nuremberg, Erlangen, Germany*

---

The goal of this study was to intraindividually compare complete versus fragmented directly labeled  $^{99m}\text{Tc}$  monoclonal anti-CEA antibody with respect to antigen targeting and tumor uptake kinetics, sensitivity and diagnostic accuracy in colorectal cancer patients. **Methods:** Twenty-five patients were investigated with  $^{99m}\text{Tc}$ -labeled anti-CEA IgG<sub>1</sub> BW 431/26 and the F(ab')<sub>2</sub>/Fab' fragment mixture F023C5 within 7 days. For quantitative analysis, an ROI technique was applied to planar scans, whole-body scans and SPECT slices 10 min to 48 hr postinjection. Final correlations were performed according to histology after surgery or biopsy. **Results:** Earliest tumor detection with complete IgG<sub>1</sub> was possible 4 hr postinjection (52% of finally positive lesions); imaging at 24 hr or even 48 hr was necessary in 48%. Tumor detection with fragments was possible in 17% at 1 hr postinjection and in 94% at 4 hr postinjection. In 35%, SPECT was necessary for tumor detection with both MAbs. Absolute antibody uptake in tumor lesions was higher with complete MAbs than with fragments. **Conclusions:** Lesions known for their good vascularization, vascular permeability and antigen accessibility were detected earlier and with higher sensitivity with fragments than with complete MAbs due to faster background clearance despite lower absolute antibody uptake.

**Key Words:** colorectal cancer; immunoscintigraphy; carcinoembryonic antigen; IgG<sub>1</sub> F(ab')<sub>2</sub>/Fab' fragments

**J Nucl Med 1995; 36:430-441**

---

Colorectal cancer is the second most common cause of cancer mortality in Europe and the U.S. (approximately 140,000 cases and 70,000 deaths per year in the U.S.) (1,2), and there has been little change in the overall mortality over the past 30 yr (3-5). For improvement, early tumor and especially recurrence detection seems crucial

(2-4,6,7). In this context, immunoscintigraphy has crossed the research/clinical barrier (8) to become a widely accepted diagnostic procedure in Europe and the U.S. with several MAbs available with  $^{123}\text{I}$ ,  $^{111}\text{In}$  and  $^{99m}\text{Tc}$ -labeled, respectively (9-15). Complete immunoglobulin molecules have rather slow kinetics with regard to tumor uptake and whole-body clearance (for overview see 14). This led to the development of fragments with a more rapid clearance (13), especially suitable for labeling with short-lived isotopes, such as  $^{99m}\text{Tc}$ . The smaller size may also reduce the HAMA response (10,14). However, in vitro studies have shown significantly diminished affinity of fragments to the antigen (16). In combination with the rapid whole-body clearance, a lower absolute antibody uptake of fragments in the tumor might be expected.

Numerous animal and clinical studies on kinetics, sensitivities, and diagnostic accuracy of whole and fragmented antibodies labeled with  $^{131}\text{I}$ ,  $^{125}\text{I}$ ,  $^{123}\text{I}$ ,  $^{111}\text{In}$  and  $^{99m}\text{Tc}$  have been conducted (10-15,17-27). There have been studies comparing different cohorts of patients or animals with different antibody fragmentation grades (28-30), but until now, no clinical imaging investigations using two different antibody fragmentation grades in the same patient have been reported. This is the very field, where animal experiments cannot deliver information of clinical significance because of the different physicochemical tumor environment (20,31-33).

In our study, we prospectively compared antibody targeting kinetics, sensitivities and diagnostic accuracy of two  $^{99m}\text{Tc}$ -labeled anti-CEA MAbs of different fragmentation grade (IgG<sub>1</sub> BW 431/26 versus a F(ab')<sub>2</sub>/Fab' mixture of clone F023C5) intraindividually. This permits direct comparison of both molecular species in the same individual and tumor, reducing several potential sources of variation between specimens. Both MAbs belong to different clones, but both recognize a related class III protein antigenic determinant of CEA according to the classification of Primus (34), with similar affinity (35,36) of their parent IgG species. Hence, a comparable behavior of both MAbs

---

Received June 16, 1994; revision accepted Nov. 11, 1994.

For correspondence or reprints contact: Wolfgang S. Becker, MD, Professor of Nuclear Medicine, Department of Nuclear Medicine, Friedrich-Alexander University of Erlangen-Nuremberg, Krankenhausstr. 12, D-91054 Erlangen, Germany.

could be expected, differences relying on the different fragmentation grade only.

## MATERIALS AND METHODS

### Patient Selection

Between November 1992 and February 1994, we prospectively investigated 25 patients with CEA expressing tumors (23 with recurrent colorectal carcinoma, 1 endometrial and 1 lung adenocarcinoma with immunohistologically proven CEA expression; Table 1). All patients had suspected recurrent or metastatic disease. The age range was 41–77 yr (mean 58.5 yr); 19 patients were male and 6 female. CEA levels ranged between 1.0 and 1178.0 ng/ml (mean 72.5 ng/ml, median 9.4 ng/ml, normal value  $\leq 5.0$  ng/ml). Within a 1-wk period, patients were studied with both  $^{99m}\text{Tc}$ -labeled antibodies in a randomized fashion. Usually, on Day 1 the first antibody was injected and 1 hr and 4- to 6-hr imaging performed. After 24-hr imaging on Day 2, the second antibody was administered with subsequent early imaging (when 48-hr scans were required, the second injection was delayed to day three). Finally on Day 3, 24-hr scanning of the second antibody was performed.

### Antibody Preparation

Both murine antibodies, belonging to the IgG<sub>1</sub> class, react with a related class III peptide antigenic determinant of the CEA molecule (34,35,37). The IgG<sub>1</sub> class antibody BW 431/26 (Behringwerke, Marburg, FRG), an extensively studied anti-CEA antibody (10,11,20,38), was directly labeled with  $^{99m}\text{Tc}$  in a two-step procedure according to Schwarz & Steinsträsser (39). Briefly, reduction to form free thiol groups was performed using a mercaptoethanol method, and the pretreated antibodies (protein content 2 mg/vial) were obtained from the manufacturer as a sterile lyophilized powder under nitrogen atmosphere with 2 mg of sorbitol as radioprotective, buffered with 2 mg of sodium phosphate. For labeling, the material was dissolved in 1 ml of a solution of 0.5 mg tetrasodium-1,1,3,3-propanetetra-phosphonate and 0.02 mg Sn(II)Cl<sub>2</sub> in 0.9% saline, to which about 1480 MBq of a fresh technetium generator eluate (0.5–2 ml) were added. After a 15 min incubation at room temperature, the solution was suitable for injection (radiochemical purity  $\geq 97\%$ ).

F023C5 (Sorin Biomedica, Saluggia, Italy) has been studied as whole IgG<sub>1</sub> and F(ab')<sub>2</sub> fragments with  $^{131}\text{I}$ ,  $^{125}\text{I}$  and  $^{111}\text{In}$ -label (15,36,40–42). Technetium-99m-labeled F(ab')<sub>2</sub> fragments were introduced recently in clinical investigation (21,43): they were prepared by enzymatic digestion and gel filtration chromatography. These F(ab')<sub>2</sub> fragments were reduced to deliver free thiol groups for Tc-labeling by a conventional pretinning method (44) and obtained from the manufacturer as a sterile and pyrogen-free lyophilized mixture under nitrogen atmosphere, consisting of 0.50 mg antibody protein, 0.02 mg stannous chloride, 2.00 mg sodium tartrate and 7.70 mg potassium phthalate. Labeling was done by dissolving the lyophilized material in 1 ml of fresh technetium generator eluate (approx. 1850–2220 MBq TcO<sub>4</sub><sup>-</sup> in 0.9% saline). After 15 min at room temperature, approximately 80%–88% of total activity was found to be protein-bound. The remaining free pertechnetate and reduced  $^{99m}\text{Tc}$  were removed by a combined gel filtration/anion exchange chromatography on a small column of DEAE Sephadex A-25 using 0.9% saline as the eluant (43).

### Antibody Molecular Species Analysis and Affinity Determination

For analysis of molecular composition, labeled antibodies were analyzed by gel filtration chromatography on a column of Sephadex G-100 Superfine (0.5 × 120 cm) as described elsewhere in more detail (45,46). Fractions were collected, analyzed for their activity in a well counter and for their protein content using a modified bicinchoninic acid procedure (MicroBCA Pierce, Rockford IL). Sodium dodecyl sulfate gel electrophoresis (SDS-PAGE) was done under nonreducing conditions as described earlier (45). Antibody affinity was determined by Scatchard plot analysis (47) as described by Bosslet et al. (35).

### Antibody Administration and Scintigraphic Protocol

A dose of 740–1295 MBq (1.5–1.9 mg of IgG, 0.3–0.5 mg of fragments) was injected intravenously within 30 min after labeling through an indwelling catheter. Whole-body scans were acquired at 10 min and 1, 4 and 24 hr postinjection. Planar imaging of the pelvis, abdomen, thorax and head was performed 4–6 hr and 18–24 hr postinjection (anterior-posterior and lateral projections). In selected cases, 48-hr scans were performed of critical regions.

SPECT of the pelvis and abdomen was performed 4–6 hr postinjection. SPECT of the thorax and a second abdomen SPECT was performed 18–24 hr postinjection. Variation of this protocol (e.g., SPECT of the head) was done depending on the clinical problem. All images were concordantly judged by three experienced nuclear medicine physicians without knowledge of the results of other imaging modalities and later compared to conventional procedures (CT, MRI, ultrasonography). In this study, positive liver metastasis delineation was defined as either: warm or hot liver lesions, i.e., a tumor/background ratio  $\geq 1.10$ , or a cold lesion with a scintigraphically hot rim or rim sign (20) if compared to normal liver parenchyma. Lesions appearing as scintigraphically isointense (i.e., tumor-to-background ratio of 0.90–1.09) or cold (tumor-to-background ratio  $\leq 0.90$ ) when compared to normal liver parenchyma were interpreted as negative (also read as negative were lesions which had some diffuse antibody uptake, but remained below physiological liver activity during the imaging course).

### Camera Equipment and Imaging Technique

A double-headed rotating gamma camera interfaced with a Microdelta Plus Computer (Siemens Gammasonics, Erlangen, Germany) was used. Images were acquired in an analog manner (MicroDot Imager, Siemens, Erlangen, Germany) and digitally in a 128 × 128 word-mode matrix (energy window 140 keV,  $\pm 10\%$ ; planar scans at 1 and 4 hr after antibody administration with 500,000 cts/view, at 24 and 48 hr with 200,000 cts/view). For SPECT, 60 planar projections in a 360° step-and-shoot technique (4–6 hr postinjection: 30 sec/view; 24 hr postinjection: 40 sec/view) were acquired in a 64 × 64 matrix. The data were processed by filtered backprojection (Butterworth filter, Nyquist frequency 0.4–0.5) and reconstructed in three planes (transaxial, coronal and sagittal).

### Additional Imaging Techniques

All patients had a chest radiograph, abdominal and chest CT and/or (if clinically indicated) MRI, as well as ultrasonography before administration of the radiolabeled antibodies. CT was performed with a Somatom DR3 CT scanner (Siemens, Erlangen, Germany): slice thickness 8 mm, with and without oral and intravenous contrast media. In those cases where CT was indecisive,

**TABLE 1**  
**Patients Examined with IgG<sub>1</sub> BW431/26 and F(ab')<sub>2</sub>/Fab' F023C5**

Patient no.	Sex	Age (yr)	CEA level (ng/ml)	Lesion	Detected by	Immunoscintigraphic result*		
						IgG1 BW431/26	F(ab') <sub>2</sub> F023C5	
1	M	63	9.7	Primary	Endoscopy	Neg	+ 4-hr pl	
				Liver met.	CT	Neg	+ 4-hr SPECT	
				Lymph node	CT	Neg	+ 4-hr pl	
2	M	41	11.6	Liver met.	IS	+ 4-hr SPECT	+ 4-hr SPECT	
3	M	72	9.0	Liver met.	CT	+ 24-hr SPECT	+ 24-hr SPECT	
4	F	59	56.5	Retroperit. bone, and muscle met.	MRI	+ 4-hr SPECT	+ 1-4 hr SPECT	
				Unspecific bowel activity (false-positive primary)				+24-hr pl
5	F	54	196.7	Liver met.	IS	+ 4-hr SPECT	+ 4-hr SPECT	
6	F	77	1.2	Locoreg. rec.	IS	+ 24-48 hr pl	+ 4-hr pl	
7	M	45	1178.0	Brain met.	CT, MRI	+ 4-hr SPECT	+ 4-hr pl	
				Lung primary		CT	+ 4-hr SPECT	+ 4-hr SPECT
8	F	63	43.0	Locoreg. rec.	IS	+ 4-hr SPECT	+ 4-hr SPECT	
				Lymph node		IS	+ 24-hr pl	1-hr pl
9	M	65	39.6	Kidney met.	CT	+ 4-hr SPECT	Neg	
				Peritoneal carc.		IS	+ 24-hr pl	+ 4-hr pl
10	M	64	1.0	Locoreg. rec.	CT	+ 4-hr pl	+ 4-hr pl	
11	M	51	11.3	Recurrence at anastomosis	Endoscopy	Neg	+ 4-hr SPECT	
				Peritoneal carc.		IS	+ 24-hr pl	+ 4/24 hr pl
12	M	50	1.5	Lymph nodes	IS	+ 4-hr pl	+ 1-hr pl	
13	M	59	5.1	Locoreg. rec.	IS	+ 4-hr SPECT	+ 4-hr pl	
				Lymph node		IS	+ 4-hr pl	+ 4-hr pl
14	M	58	4.3	Locoreg. rec.	IS	+ 4-hr SPECT	+ 4-hr SPECT	
				Liver met.		CT	+ 24-hr pl	+ 4-hr SPECT
				Lymph node		IS	+ 24-hr SPECT	+ 4-hr SPECT
15	M	55	67.0	Locoreg. rec.	CT	+ 24-hr SPECT	+ 4-hr pl	
				Liver met.		CT	+ 24-hr pl	Neg
16	M	68	3.8	Locoreg. rec.	CT	+ 4/24 hr SPECT	1-hr pl	
17	F	54	60.0	Locoreg. rec.	CT	+ 4-hr SPECT	+ 4-hr SPECT	
				Peritoneal carc.		IS	+ 24-hr pl	+ 4/24 hr pl
18	M	54	3.4	Locoreg. rec.	IS	+ 4-hr SPECT	+ 4-hr pl	
				Lymph node		CT	+ 24-hr pl	+ 4-hr pl
19	M	64	3.9	Lung met.	CT	+ 24-hr SPECT	Neg	
20	F	63	15.0	Liver met.	CT	+ 4-hr pl	Neg	
21	M	53	59.4	Lymph node	IS	+ 24-hr pl	+ 4-hr pl	
				Locoreg. rec.		IS	+ 48-hr pl	+ 4-hr SPECT
				Peritoneal carc.		IS	+ 24-hr pl	+ 4-hr pl
22	M	54	7.8	NSAID inj. site (false-positive bone met.)		+ 4-hr pl	+ 1-hr pl	
				Locoreg. rec.		CT	+ 4-hr SPECT	+ 4-hr pl
23	M	65	3.7	Locoreg. rec.	CT	+ 4-hr SPECT	+ 4-hr pl	
24	M	76	14.0	Inflammatory tissue (false-positive locoreg. recurrence)				
				suspected from		CT	+ 4-hr pl	Doubtful
25	M	60	5.4	Lymph node	IS	? 24-hr SPECT	+ 24-hr pl	
				Liver met.		CT	+ 4-hr SPECT	+ 1-hr SPECT
				Lymph node		IS	+ 24-hr pl	? 24-hr pl

\*Time postinjection and method (planar/SPECT) which could detect tumorous lesion first. pl = planar

but immunoscintigraphy revealed tumorous lesions, additional MRI was performed.

### Laboratory Examinations

All patients had routine baseline blood chemistry measurements before antibody administration. In cases with prior exposure to murine antibodies, human anti-mouse antibody (HAMA) titers were determined in patient sera using a commercially available ELISA kit (ImmuSTRIP HAMA™, Medac, Hamburg, Ger-

many/Immunomedics Inc., Morris Plains, NJ; normal titer ≤0.200 μg/ml). In all patients, CEA serum levels were determined by a standard EIA procedure (Abbott CEA-EIA Monoclonal One-Step™, Abbott, Wiesbaden, Germany; normal range ≤5 ng/ml).

### Whole-Body and Serum Clearance Determinations

For determination of the whole-body clearance and organ uptake kinetics, an ROI technique was applied to whole-body scans

obtained 10 min, 1 hr, 4 hr and 24 hr after antibody administration (calculation of the geometric mean, physical half-life correction, expression in percent of injected dose by referring to whole-body counts at 10 min after MAb injection). Absolute tumor uptake in lymph node metastases was calculated by applying the ROI technique to the peripheral lymph node metastases of three patients (Patients 8, 12, 13; Table 1) that were visible on planar scans and had been surgically removed and weighed.

One milliliter serum samples taken 10 min, 1 hr, 4 hr and 24 hr after antibody injection were measured in a well counter to determine serum clearance. Molecular weight species composition was analyzed by gel filtration chromatography, essentially as described for native MAbs (see section Antibody Molecular Species Analysis) and as will be published elsewhere (45,46).

### Surgical Protocol and Histopathological Evaluation

Following immunoscintigraphic assessment, surgery and/or biopsy of all lesions (with exception of the brain metastasis of Patient 7, Table 1) was done within 4-wk. All specimens were examined histopathologically and also stained immunohistologically with anti-CEA antisera. Therefore, final correlation as true-positive/negative or false-positive/negative was performed according to the histopathological result.

## RESULTS

### Molecular Composition, Antigen Affinity, Serum and Whole-Body Clearance and Organ Distribution of Antibody Species

IgG<sub>1</sub> BW 431/26 was shown by SDS-PAGE and gel filtration chromatography to consist of a single-protein molecule of about 150 kD which contained more than 97% of the total Tc label, which is consistent with a Tc-labeled IgG<sub>1</sub> molecule. In contrast, F(ab')<sub>2</sub> F023C5 after Tc-labeling was demonstrated to contain two molecular weight species, presumably due to reductive disulfide bond fission during the pretinning procedure (45,48-50). Twenty-one percent of the protein had a molecular weight of about 100 kD, 79% of 50 kD, which is compatible with F(ab')<sub>2</sub> and Fab' fragments, respectively (activity based ratio Fab'/F(ab')<sub>2</sub>: 2.45:1.00).

The affinity constant of <sup>99m</sup>Tc-labeled IgG BW 431/26 was determined by Scatchard plot analysis as  $5 \times 10^9$  liter/mol good accordance with the literature (35), the affinity of <sup>99m</sup>Tc-labeled fragments F023C5 was found as  $8 \times 10^8$  liter/mol.

As expected, serum clearance of the fragment mixture was significantly higher ( $p < 0.001$ ) than that of complete antibodies (Fig. 1; biological serum  $T_{1/2}$  of IgG approximately 36 hr,  $T_{1/2}$  of F(ab')<sub>2</sub> 16 hr, Fab' 4 hr). Comparison of organ distribution and uptake of both MAbs revealed clear differences (Figs. 2, 3). With whole IgG<sub>1</sub>, liver uptake is predominant ( $15.6 \pm 4.7\%$  of injected activity 24 hr postinjection for IgG<sub>1</sub> versus  $8.2 \pm 3.8\%$  of fragments;  $p < 0.01$ ), whereas there is a marked renal antibody uptake of fragments ( $9.8 \pm 4.2\%$  for IgG<sub>1</sub> versus  $17.2 \pm 7.2\%$  for F023C5;  $p < 0.01$ ). The gallbladder was visualized with fragments F023C5 in most cases after 24 hr with SPECT and occasionally on planar scans. With complete IgG<sub>1</sub>, this observation was never made. There was a marked colonic

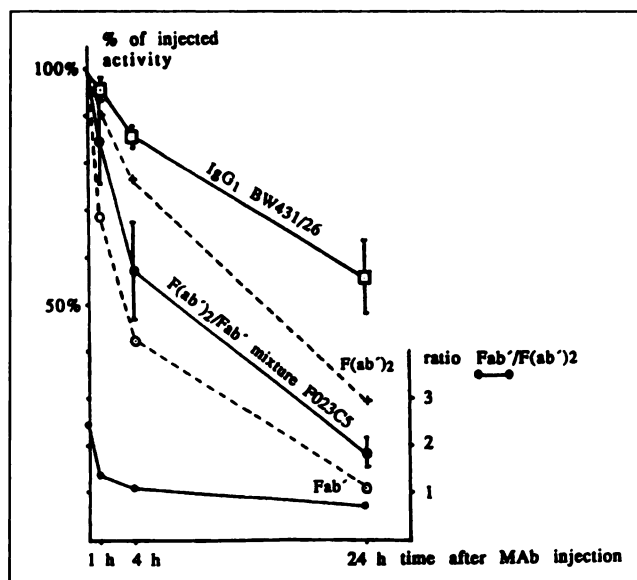


FIGURE 1. Blood serum clearance of IgG<sub>1</sub> BW 431/26 and fragments F023C5 (mixture F(ab')<sub>2</sub>/Fab', and its individual components).

mucosa visualization in 24-hr images, especially with fragments, which was somewhat lower with whole IgG (Fig. 2). The differential diagnosis of a colonic primary tumor was rather difficult at times when there was circumferential colonic MAb accumulation.

### Antibody Targeting of Tumorous Lesions

A summary of all 25 patients is given in Table 1. Overall, 2 primary tumors, 11 local recurrences, 9 patients with lymph node metastases, 8 patients suffering from liver metastases, 1 kidney metastasis, 1 brain metastasis patient and 4 peritoneal carcinomatoses were investigated. With whole IgG BW 431/26 antibodies, earliest possible tumor detection was at 4 hr postinjection (52% of lesions becoming finally positive), while in 48% 24 hr or even 48 hr scans were necessary. In 52%, SPECT was necessary for earlier detection of lesions than was possible from the planar scans, and 35% of the lesions were visualized only by SPECT. With fragments, however, tumor detection was possible in 17% of finally positive lesions at 1 hr postinjection, and at 4 hr 94% of the lesions were detected. For earliest possible tumor visualization, in 60% planar scans were sufficient, while in 40% early diagnosis required SPECT; 34% of the lesions could only be detected by SPECT.

### Overall Diagnostic Accuracy

In the 25 double studies, only three false-positive lesions were observed. In Patient 4 (Table 1), a strong antibody accumulation in the cecal pole occurred 24 hr postinjection with both MAbs and was interpreted as a colonic primary. No adequate lesions (not even inflammation) could be verified by endoscopy. The second false-positive lesion was a

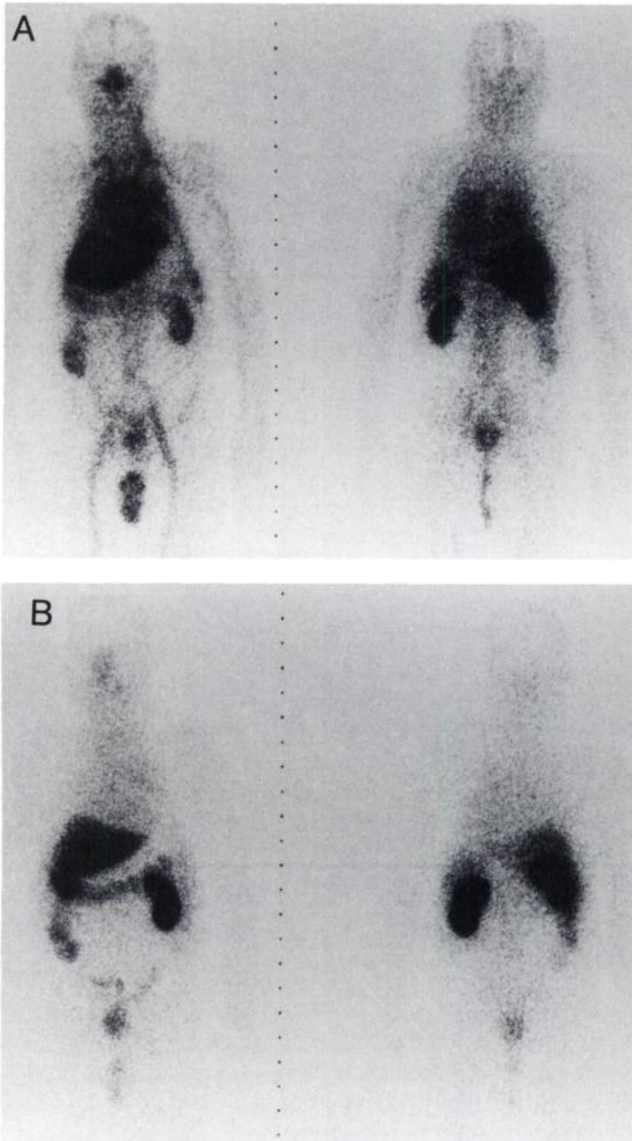


**FIGURE 2.** Normal antibody distribution (Patient 23) 24 hr postinjection. (A) IgG<sub>1</sub>. There is prominent liver uptake, high residual blood-pool activity in the heart and slight colonic mucosa uptake. In the dorsal view, locoregional recurrence is faintly visible. (B) Fragments. There is predominant renal uptake, almost no residual blood-pool activity and strong colonic mucosa delineation. In the dorsal view, locoregional recurrence is faintly visible.

nonspecific antibody accumulation at the site of intramuscular injections of NSAIDs in the gluteal muscle (Patient 22), taken false-positively as bone metastasis. The third (Patient 24) had a retrovesical soft-tissue mass strongly suspected as locoregional recurrence by CT that was interpreted as positive with the complete MAb. Fragment imaging results were doubtful and histology revealed only nonspecifically inflamed scar tissue.

## ANALYSIS BY TUMOR SITES

### Locoregional Recurrence

A total of eleven patients suffering from local recurrence were investigated in our study (Table 2, Fig. 4). Overall, all 11 local relapses were detected with F023C5, and only 9 with BW 431/26. Planar scans were more often sufficient with fragments than with IgG (5/11 versus 1/11 cases at 4 hr postinjection, 8/11 versus 6/11 cases at 24 hr postinjection), and detection was possible earlier (10/11 fragment scans at 4 hr postinjection, in comparison to 2/11 IgG scans, where 48 hr imaging was necessary; Fig. 4).

In all cases with single retrovesical recurrence with only local lymph node involvement, serum CEA levels were normal (Table 2). Six of the 11 local recurrences (all histologically confirmed) were detected only by immunoscintigraphy, while the CT scan was interpreted as normal (5/11) or had not been performed (one case). One false-positive result was observed (Patient 24, where CT had strongly suspected locoregional recurrence, IgG was interpreted as positive, fragments as doubtful). Therefore, diagnostic accuracy of F023C5 was 92% versus 67% in BW431/26 (statistically significant,  $p < 0.05$ ).

### Liver Metastases

When comparing both MAbs in liver metastases targeting, clear differences in sensitivity in dependence of lesion size became evident (Table 3). Small liver lesions (<2 cm) could be detected with similar sensitivity as scintigraphically hot with both MAbs (8/8 versus 7/8 lesions with F023C5 and BW 431/26 each;  $p > 0.05$ ). Medium-size lesions (2–4 cm in diameter) were detectable with higher sensitivity when using fragments (5/5 versus 2/5;  $p < 0.05$ ).

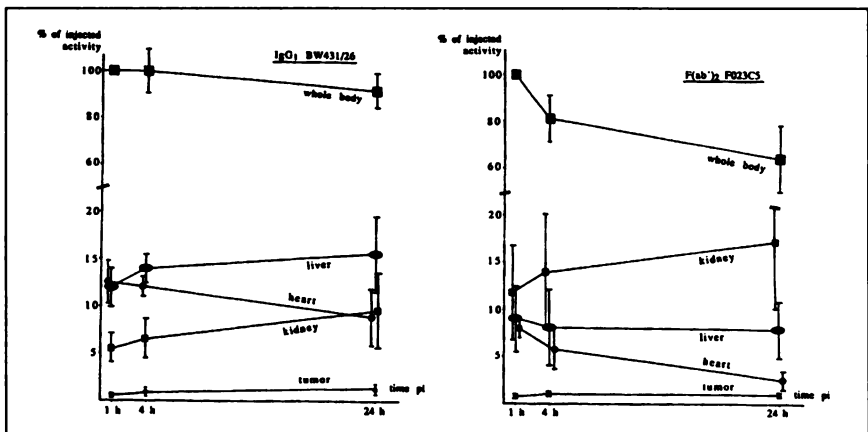


**FIGURE 3.** Organ and whole-body kinetics of IgG and fragments. Tumor means approximately 10 g of lymph node metastasis tissue (mean  $\pm$  s.d. taken from three patients).

**TABLE 2**  
Locoregional Recurrence Detection with IgG1 BW431/26 and F(ab')<sub>2</sub>/Fab' F023C5

Patient no.	CEA level (ng/ml)	Stage at time of surgery of primary (TNM classif.)	Time after surgery of primary	Size of locoregional recurrence (cm)	IgG1 pl.		SPECT 4 hr	Fragmented pl.		SPECT 4 hr	First detected by
					4 hr	24 hr		4 hr	24 hr		
6*	1.2	T2 N0 M0	7 yr	4.1	-	(+)	(+)	+	+	+	IS
8	43.0	T3 N1 M0	10 mo	4.5	-	(+)	+	-	-	+	IS
10*	1.0	T3 N2 M0	3 yr 1 mo	2.7	+	+	+	+	+	+	CT
13*	5.1	T2 N0 M0	5 yr 3 mo	2.5	-	(+)	+	+	+	+	IS
14	4.3	T2 N0 M0	2 yr 8 mo	3.0	-	+	+	-	+	+	IS
15	67.0	T3 N2 M0	1 yr	3.1	-	-	(+)	+	+	+	CT
16*	3.8	T3 N0 M0	3 yr 2 mo	2.3	(+)	+	(+)	(+)	+	(+)	CT
17	60.0	T3 N2 M0	2 yr 4 mo	7.5	(+)	+	+	(+)	+	+	CT
18	3.4	T4 N2 M0	8 mo	6.2	-	+	+	(+)	(+)	+	IS
21	59.4	T3 N0 M0	8 mo	3.1	-	(+)	+	(+)	+	+	IS
23*	3.7	T3 N2 M0	5 yr 1 mo	5.1	(+)	+	+	+	(+)	(+)	MRI
False-positive: histological scar tissue with unspecific inflammatory infiltration, strongly suspected by CT as recurrence:											
24	14.0	T1 NxMx	7 mo	2.5	-	(+)	+	-	-	(+)	CT false-pos.

\*Patients with locoregional recurrence with not more than local lymph node involvement as single tumor recurrence manifestation.  
- negative; + positive scan interpretation; (+) doubtful

With whole IgG<sub>1</sub>, these lesions were indistinguishable from normal liver parenchyma (interpreted as negative, see Materials and Methods). Large metastases appeared as scintigraphically isointense or cold when using fragmented MABs, whereas with whole IgG, they developed a hot rim or rim sign (20) within 24 hr. These larger lesions took up fragmented antibody protein more homogeneously and diffusely, generally remaining colder than normal liver parenchyma.

The overall sensitivity in liver metastasis detection was therefore higher for fragments (13/15 versus 11/15), but tumor-to-liver background ratios of scintigraphically

positive lesions were significantly higher with IgG than with fragments (Figs. 5, 6):  $1.70 \pm 0.32$  versus  $1.26 \pm 0.12$  ( $p < 0.01$ ) (values at time of maximal tumor-to-background ratio, usually 24 hr postinjection with IgG<sub>1</sub>, 4 hr postinjection with fragments). The cutoff for positive liver lesion delineation was defined at 1.10 (specific uptake higher than normal liver tissue), but the unequivocal blinded interpretation as positive without knowledge of the CT scan result was possible at tumor-to-background ratios above 1.25. Only 7/13 positive liver metastases fulfilled this requirement with fragments, compared to 11/11 with IgG<sub>1</sub>. The fact that only one liver

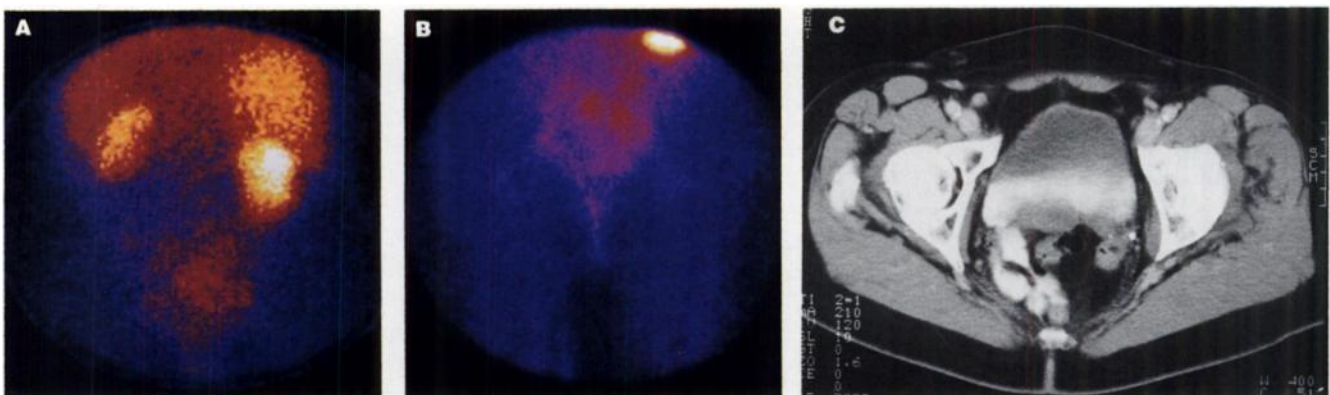


**FIGURE 4.** Locoregional recurrence visualization in dependence of time after antibody administration in Patient 6, with sacral pain but normal CT scan (local recurrence confirmed by surgery). (A) BW 431/26 planar, dorsal view of the abdomen 48 hr postinjection shows antibody accumulation in the sacral region (earlier scans being negative). (B) F023C5 planar, dorsal view of the pelvis, 4 hr postinjection; clear visualization of local recurrence. (C) CT scan without sign of local recurrence.

**TABLE 3**  
Liver Metastases: Immunoscintigraphic Results Based on Size

Patient no.	CEA level (ng/ml)	Lesion localization	Size (cm)	Immunoscintigraphic result				
				IgG1 SPECT	BW431/26 pl	F(ab)'2 SPECT	F023C5 pl	
<b>Small liver metastases (&lt;2 cm in diameter)</b>								
2	11.6	a	segm VI/VII	1.6	4-hr	24-hr	4-hr	(24-hr)
		b	segm VI	0.6	—*	—	4-hr	—
		c	segm VI	1.2	4-hr	24-hr	4-hr	—
5	196.7	a	segm VII	1.0	4-hr	—	4-hr	—
		b	segm VII	1.1	4-hr	—	4-hr	—
		c	segm VIII	1.3	4-hr	—	4-hr	—
14	4.3	a	segm VI	0.9	24-hr	24-hr	4-hr	—
15	67.0	a	segm VII	1.0	24-hr	—	15-hr	—
				Sensitivity	7/8	3/8	8/8	(1)/8
<b>Medium size liver metastases (2–4 cm in diameter)</b>								
1	9.7	a	segm V	2.8	—*	—	4-hr	—
		b	segm VI	3.0	—*	—	4-hr	—
		c	segm VIII	2.9	—*	—	4-hr	—
3	9.0	a	segm VI	4.0	24-hr	—	24-hr	—
25	5.4	a	segm VI	3.9	4-hr	24-hr	1-hr	24-hr
				Sensitivity	2/5	1/5	5/5	1/5
<b>Large liver metastases (&gt;4 cm in diameter)</b>								
15	67.0	b	segm VI/VII	5.9	24-hr†	24-hr	—*	—
20	15.0	a	segm VI/VII	4.2	4-hr†	4-hr	—*	—
				Sensitivity	2/2	2/2	0/2	0/2
					11/15	6/15	13/15	1/15

\*Indistinguishable from normal liver parenchyma (i.e., tumor-to-background ratio 0.90–1.09). †Scintigraphically cold with surrounding "hot" rim. ‡Scintigraphically cold when compared to normal liver parenchyma (i.e. tu./backgr. ratio ≤0.90).

lesion was seen in planar scans with fragments (Table 3) in comparison to 6/15 with IgG at 24 hr after antibody administration is easily explained by these lower ratios (Fig. 5).

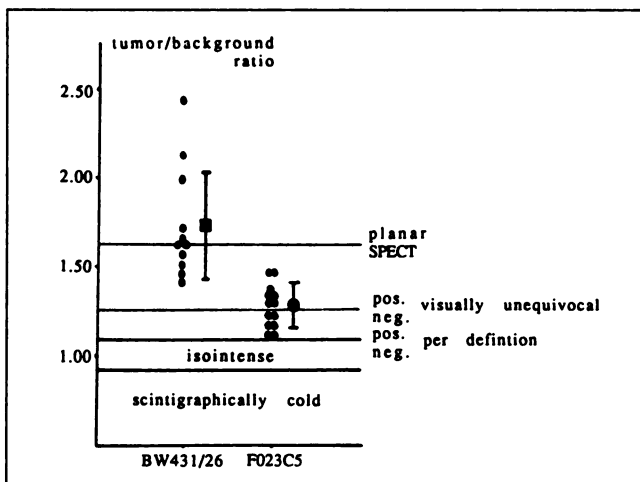


**FIGURE 5.** Tumor-to-background ratios of scintigraphically positive (i.e., tumor-to-background ratio >1.10) liver metastases with IgG and fragments.

### Lymph Node Metastases

Lymph node metastasis detection was possible with fragmented MAb earlier after injection and with higher sensitivity when compared to complete antibodies (Table 4). The overall sensitivities of fragments versus whole IgG<sub>1</sub> were 9/9 (100%) versus 6/9 (67%), respectively ( $p < 0.05$ ). Positive lesion detection was possible earlier with fragments (2/9 at 1 hr postinjection, 7/9 at 4 hr postinjection, compared to only 1/9 at 4 hr postinjection with IgG), and in a higher percentage, planar scans were sufficient (8/9 versus 3/9). When examining antibody uptake kinetics in lymph node metastases (see above), a clear trend was observable. Absolute protein uptake is lower with fragments, but rapid background clearance leads to faster tumor delineation, mostly on planar scans. The greatest uptake occurs in the first 4 hr after antibody administration of fragments, while uptake is continuous over 24 hr with IgG<sub>1</sub> (1 hr postinjection:  $0.5 \pm 0.2$  versus  $0.6 \pm 0.2$ ; 4 hr postinjection:  $0.7 \pm 0.4$  versus  $0.7 \pm 0.2$ ; 24 hr postinjection:  $1.1 \pm 0.6$  versus  $0.6 \pm 0.3$ ; values in %ID/10 g for IgG<sub>1</sub> versus fragments;  $n = 3$ ; no statistical significance given because of low number available).

### Peritoneal Carcinomatosis

The typical feature of diffuse peritoneal carcinomatosis was seen in four patients. Diffuse delineation of the whole

peritoneal cavity and especially the peritoneal wall, forming a typical u-like activity accumulation (51) (Fig. 7), was clearly discernable with fragments in all cases beginning 4 hr after antibody administration; the results were unequivocally positive after 24 hr. With complete IgG, 24-hr scans became positive, but they were not as impressive as the images obtained with fragments (higher nonspecific background, Fig. 7).

#### **Single Cases: Primary Tumors, Kidney, Lung, Bone and Brain Metastases**

Table 4 summarizes imaging results of single cases. One colonic primary tumor could be exclusively detected by fragments (Patient 1, 4 hr postinjection, planar and SPECT). A kidney metastasis was seen with fragments as a cold hole (SPECT 4 hr postinjection: ratio metastasis/normal kidney parenchyma: 0.42) in the kidney parenchyma; with complete IgG, however, 4 hr SPECT was clearly positive with a tumor-to-background ratio of 1.27.

Patient 19 had a lung metastasis (2 cm in diameter) in the right lower lobe which was negative with fragments. It became faintly positive in SPECT with complete IgG<sub>1</sub> after 24 hr postinjection. One bone metastasis (Patient 4 with a spine lesion) was delineated as positive with both MAbs, with the fragmented antibody as early as 1 hr after injection, with IgG not before 4 hr postinjection (SPECT). Patient 7 suffered from two brain metastases due to occult nonsmall-cell lung cancer with diffuse mediastinal lymph node involvement as well. One metastasis in the right parieto-occipital lobe measured 2.5 cm in diameter, and the other in the cerebellopontine region measured only 0.4 cm; both MAbs were positive for the larger metastasis, but negative for the smaller one (fragments in planar scans, IgG only in SPECT).

#### **Previously Unsuspected Lesions**

In 56% (14 patients) of the 25 patients, previously unsuspected lesions were found (Table 1). No significant differences in frequency of detection of previously unsuspected lesions were noticed between both MAbs. Two patients with previously unknown liver metastases, six locoregional recurrences, six patients with lymph node metastases and four peritoneal carcinomatoses were detected. This information would, according to the referring surgeons, influence the therapeutic regimen in 32% (8/25) of patients. In three patients (2, 6 and 8; Table 1) identified lesions were surgically removed; external beam radiation and/or chemotherapy was given in five patients (5, 9, 13, 17, 18; Table 1), avoiding surgery in three (9, 13, 17) of these patients, where the true extent of disease had been underestimated by conventional methods, and surgery had no chance of curativity any longer.

#### **DISCUSSION**

To our knowledge, this is the first time that tumor targeting kinetics, sensitivity and diagnostic accuracy have been investigated using MAbs of different fragmentation sizes in the same patient under imaging conditions. The

study of different lesion sites with their complex and different pathophysiological characteristics seems possible only in the human situation. Animal models cannot mimic these individual sophisticated conditions (i.e., vascularization, vascular permeability, interstitial pressure.) (31–33).

Both antibodies are probably directed against different peptide epitopes (35,37) on the CEA molecule, since they derive from different hybridoma clones. We believe that the results are nevertheless valid. The antigen affinity of the parent MAb (IgG<sub>1</sub>) of both could be demonstrated to be similar (the affinity of fragments being about 15% of a complete IgG is a well known phenomenon (16)); both are directed against a related class III peptide determinant of carcinoembryonic antigen (34) and hence, no fundamental differences with exception of molecular weight should interfere. They are the only <sup>99m</sup>Tc-labeled anti-CEA MAbs in use and approved for routine diagnosis in Europe, so they alone were available for the routine diagnostic work-up of patients under clinical, nonexperimental conditions.

Both MAbs were directly labeled with <sup>99m</sup>Tc. Whole IgG<sub>1</sub> BW 431/26 was still a homogenous 150 kD protein after labeling, the F(ab')<sub>2</sub> fragments of F023C5 are further fragmented essentially to Fab' by the reductive step of the labeling procedure, which is a well known phenomenon inherent to conventional direct <sup>99m</sup>Tc-labeling procedures (44–46, 48–50).

Whereas liver uptake was predominant with IgG, presumably through Fc receptor-mediated uptake (52) and nonspecific protein catabolism, renal uptake with fragments results from glomerular filtration and tubular reabsorption with subsequent storage of fragments and their metabolites (46). As was observed for other anti-CEA MAb fragments (53), there is a biliary excretion pathway for the fragments or their metabolites (46) not seen for IgG (important differential diagnosis to liver metastases). It remains unclear whether the colonic mucosa delineation is caused by nonspecific stool activity through biliary excretion or, since this phenomenon is common to both MAbs, due to specific MAb uptake at CEA expressed on the surface of colonic mucosa cells. Slight reactivity of both MAbs with normal mucosa could be demonstrated immunohistologically (35,37).

As expected from earlier studies (11–15,24), the overall sensitivities were higher with fragments than with complete IgG. Positive tumor detection was possible in 17% as early as 1 hr postinjection of fragments. For IgG, however, 24-hr imaging was essential and some lesions were not visualized before 48 hr postinjection. Such late imaging is very difficult with radionuclides with short physical half-lives, such as <sup>99m</sup>Tc (to acquire 200,000 cts at 48 hr postinjection, acquisition times of 30–45 min for a single view must be taken into account). Their higher sensitivity at earlier time-points probably results from the known (14,31–33) ability of fragments to diffuse and penetrate more easily into tissue and to be cleared faster from blood and nonspecific background, yielding higher tumor-to-background ra-

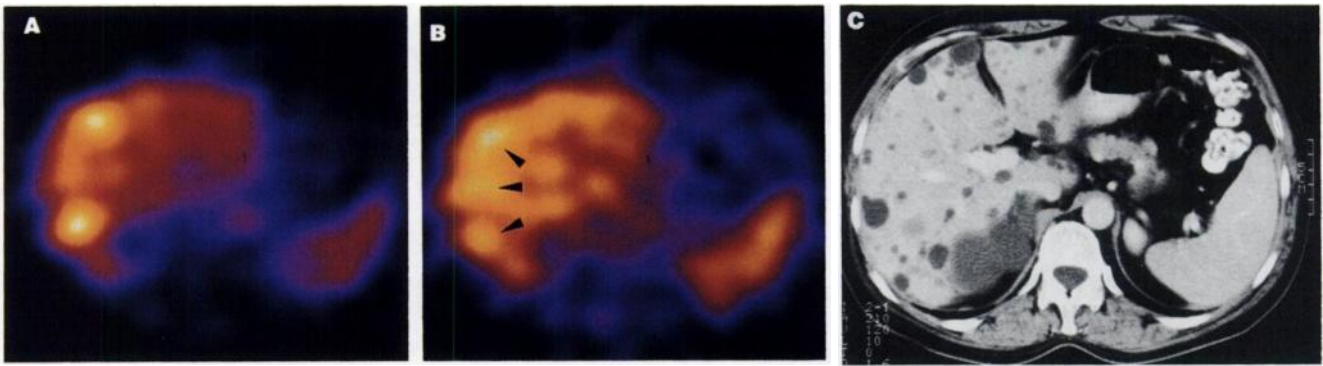


**FIGURE 6.** Liver metastases in Patient 2, with polycystic liver and kidney disease, where neither CT nor MRI could reliably differentiate between cystic and metastatic lesions. (A) IgG SPECT 4 hr postinjection shows two clearly hot metastases. (B) Fragments SPECT 4 hr postinjection shows three metastases appearing as warm (arrows). (C) CT slice in the same plane as (A) and (B). Multiple round liver lesions, most of them are cysts. Only the three lesions which were positive in the CEA scan were histologically proven to be metastatic.

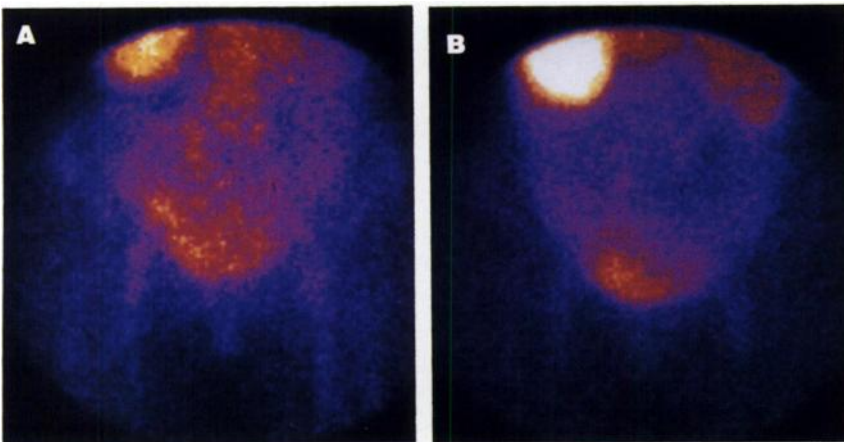


**FIGURE 7.** Large local recurrence and peritoneal carcinomatosis (Patient 17; peritoneal carcinomatosis previously unknown, histologically confirmed). (A) IgG 24 hr postinjection. Anterior view of the abdomen. There is huge antibody accumulation in the recurrence and faint delineation of the peritoneal cavity. (B) Fragments 24 hr postinjection. Anterior view of the abdomen. In addition to the recurrence, there is u-like activity accumulation in the peritoneal cavity.

**TABLE 4**  
Overall Sensitivities of IgG versus Fragments

	IgG				Fragments			
	Overall sensitivity	Planar		SPECT	Overall sensitivity	Planar		SPECT
		4 hr	24 hr	4 hr		4 hr	24 hr	4 hr
Local rec.	9/11	1	6 2 <sup>48 hr</sup>	8	11/11	5	8	9 11 <sup>24 hr</sup>
Liver met.	11/15	1	6	7 11 <sup>24 hr</sup>	13/15	0	1	12 13 <sup>24 hr</sup>
Lymph nodes	6/9	1	3	1 6 <sup>24 hr</sup>	9/9	7 2 <sup>1 hr</sup>	8	7 9 <sup>24 hr</sup>
Perit. carc.	4/4	0	4	N/A*	4/4	4	4	N/A*
Primary tumor	0/1	0	0	0	1/1	1	1	1
Kidney met.	1/1	0	0	1	0/1	0	0	0 <sup>†</sup>
Lung met.	1/1	0	0	1 <sup>24 hr</sup>	0/1	0	0	0
Bone met.	1/1	0	1	1	1/1	1 <sup>1 hr</sup>	1	1
Brain met.	1/2	0	0	1	1/2	1	1	1

\*Diagnosis of peritoneal carcinomatosis usually performed from planar scans.

†Cold lesion in hot kidney parenchyma.

tios more rapidly. However, the absolute antibody uptake was significantly less than with whole IgG.

Early locoregional recurrence detection is a severe problem of conventional imaging procedures (5,54). Because of its poor prognosis (55), detection as early as possible is critical. CEA serum levels, however, have been proven to be too insensitive, as was shown by Moertel et al. (56) and this study as well. Despite the primarily renal excretion of fragments and their metabolic products, their sensitivity in the detection of retrovesical locoregional recurrence was found to be higher than that of IgG. Obviously, the more rapid background fading with resulting higher tumor-to-background ratio overcomes problems of urinary bladder activity.

The definition of positive liver metastasis detection in immunoscintigraphy is controversial in the literature (10,20,38,46). Some authors (38) interpret every liver abnormality in an antibody scan as metastasis, whether the image is scintigraphically cold, warm or with a hot rim. We do not agree with this view. Cold lesions could be cysts, benign liver tumors or metastases from non-CEA expressing tumors (20,46). Hence, only tumor-to-background ratios above 1.10 (either homogeneously or rim signs) were interpreted as positive. Several studies have shown low sensitivities for liver metastasis detection with whole antibodies (20) because of slow diffusion of large molecules into tissue of high interstitial pressure with poor blood supply (31-33). The reported higher sensitivities of fragments (13,43,57) were demonstrated with this study as well. However, the absolute antibody uptake and the tumor-to-background ratios of fragments were significantly lower for several reasons. First, the blood clearance of fragments is so fast that only a short time exists for diffusion of molecules into the lesions with high interstitial pressure (31,32,46). Whole IgG has a longer residence in blood. Hence, in time, more antibody is exposed to the antigen-expressing cells to reach a significantly higher protein uptake per tumor weight unit. Second, the affinity of Fab' fragments is significantly lower than of IgG<sub>1</sub> (16). Scintigraphically unequivocal positive metastasis detection (without knowledge of CT scan results) could be defined at a tumor-to-background ratio greater than 1.25. Only about 50% of positive liver metastases reach this level in fragment studies (cf. Fig. 5). Despite the higher sensitivity of fragments, neither IgG nor Fab' seems to be the ideal agent for liver lesion imaging. Perhaps real F(ab')<sub>2</sub> could meet all requirements: less nonspecific liver parenchymal uptake (52) and more rapid kinetics than whole IgG (46), a longer residence time in the blood than Fab' so that slow diffusion kinetics are possible (32,46) and a similar antigen affinity as complete IgG (16).

Immunoscintigraphy was found to deliver additional information to conventional imaging methods. In 56% of patients, previously unsuspected lesions were detected. Because of the different advantages of complete or fragmented MABs imaging, depending on different tumor localizations, subsequent investigations with whole and frag-

mented MAB seem advisable in critical cases, such as rising CEA levels without any obvious reason. The authors do not recommend the administration of a cocktail because the slow background clearance of the IgG component would annihilate early tumor visualization by fragments. For the concrete clinical situation, the authors propose initially imaging with fragments because of their higher general sensitivity in the time frame available with <sup>99m</sup>Tc (and also because of their known lower HAMA induction rate (10,14) and there are no limits on further immunoscintigraphic investigations or jeopardizing in-vitro serum parameter determinations). In case of negative or doubtful results, a trial with complete IgG (including 24-hr SPECT and eventually 48-hr planar imaging of selected regions) seems useful.

In conclusion, our comparative study shows that fragments are more suitable than whole IgG molecules for rapid and reliable diagnosis of most tumor sites because positive tumor detection is possible with higher tumor-to-background ratio in most cases after 1-4 hr following injection. With lesions of poor perfusion and high interstitial pressure (e.g., hepatic and lung metastases), the situation is more difficult because the sensitivity of fragments to detect liver lesions is higher than that of IgG. In this context, the recent development of stable, directly labeled <sup>99m</sup>Tc F(ab')<sub>2</sub> fragments seems promising (58,59) because they combine the advantages of both IgG and Fab' antibodies.

#### ACKNOWLEDGMENTS

The authors thank Dr. A. Steinsträsser, Behringwerke, Frankfurt, FRG, for providing the CEA-expressing colon carcinoma cell line CaCa2 for affinity determination of both monoclonal antibodies, and Dr. E. Hannappel and Dr. W. Fischer, both of the Institute of Biochemistry of the Faculty of Medicine of the University of Erlangen-Nuremberg, FRG, for providing valuable advice about in vitro examinations. The authors also thank Mr. Robert M. Dunn, MS, Newark, NJ, for his expert help in preparing the manuscript.

#### REFERENCES

1. Kinsella AR. *Colorectal cancer: a scientific perspective*. Cambridge, England: Cambridge University Press 1993:27-53.
2. Alabaster O. Colorectal cancer: epidemiology, risks and prevention. In: Ahlgren JD, Macdonald JS, eds. *Gastrointestinal oncology*. Philadelphia, PA: Lippincott; 1992:237-259.
3. Schatzkin A, Schiffman MH. Etiology and prevention: the epidemiologic perspective. In: Wanebo HJ, ed. *Colorectal cancer*. St. Louis, MO: Mosby; 1993:3-19.
4. Müller BA, Ries LAG, Hankey BF, Kosary CL, Edwards BK, eds. *Cancer statistics review 1973-1989*; NIH Pub. No. 92-1789. Rockville, Md: National Institutes of Health, National Cancer Institute; 1992.
5. McDermott FT, Hughes ESR, Pihl E, Johnson WR, Price AB. Local recurrence after potentially curative resection for rectal cancer in a series of 1008 patients. *Bri J Surg* 1985;11:478.
6. Klapdor R. Früherkennung des kolorektalen Karzinoms. *Dtsch Med Wschr* 1989;114:262-265.
7. Dukes CE, Bussey HJR. The spread of rectal cancer and its effect on prognosis. *Br J Cancer* 1985;11:478.
8. Serafini AN. Monoclonal antibody imaging: crossing the research/clinical barrier [Letter]. *Semin Nucl Med* 1993;23:88.
9. Schlom J. Innovations in monoclonal antibody tumor targeting. *JAMA* 1989;261:744-746.

10. Becker W, Bair HJ, Behr T, Wolf F. Indikationen zur immunszintigraphie bei entzündlichen erkrankungen und beim kolorektalen karzinom. *Der Nuklearmediziner* 1994;17:251-272.
11. Reilly RM. Immunoscintigraphy of tumours using <sup>99m</sup>Tc-labeled monoclonal antibodies: a review. *Nucl Med Commun* 1993;14:347-359.
12. Galandiuk S. Immunoscintigraphy in the surgical management of colorectal cancer. *J Nucl Med* 1993;34:541-544.
13. Goldenberg DM, Wlodowski TJ, Sharkey RM, et al. Colorectal cancer imaging with iodine-123-labeled CEA monoclonal antibody fragments. *J Nucl Med* 1993;34:61-70.
14. Goldenberg DM. Monoclonal antibodies in cancer detection and therapy. *Am J Med* 1993;94:297-312.
15. Siccardi AG, Buraggi GL, Callegaro L, et al. Immunoscintigraphy of adenocarcinomas by means of radiolabeled F(ab')<sub>2</sub> fragments of an anti-carcinoembryonic antigen monoclonal antibody: a multicenter study. *Cancer Res* 1989;49:3095-3103.
16. Fjeld JG, Michaelsen TE, Nustad K. The binding parameters of radiolabelled monoclonal F(ab')<sub>2</sub> and Fab' fragments relative to immunoglobulin G in reactions with surface-bound antigen. *Eur J Nucl Med* 1992;19:402-408.
17. Patt YZ, Lamki LM, Shanken J, et al. Imaging with In-111-labeled anti-carcinoembryonic antigen monoclonal antibody ZCE-025 of recurrent colorectal or carcinoembryonic antigen-producing cancer in patients with rising serum carcinoembryonic antigen levels and occult metastases. *J Clin Oncol* 1990;8:1246-1254.
18. Moffat FL, Vargas-Cuba RD, Serafini AN, et al. Radioimmunodetection of colorectal carcinoma using technetium-99m-labeled Fab' fragments of the IMM-4 anti-carcinoembryonic antigen monoclonal antibody. *Cancer* 1994;73:836s-845s.
19. Goldenberg DM. Radiolabeled antibodies. *Scientific American Science & Medicine* 1994;1:64-73.
20. Bock E, Becker W, Scheele J, Wolf F. Diagnostic accuracy of <sup>99m</sup>Tc-anti-CEA immunoscintigraphy in patients with liver metastases from colorectal carcinoma. *Nuklearmedizin* 1992;31:80-83.
21. Mariani M, Bonino C, Tarditi L, et al. Early clinical results with Tc-99m-labeled F(ab')<sub>2</sub>. In: Epenetos A, ed. *Monoclonal antibodies: applications in clinical oncology*. London: Chapman & Hall 1991:297-308.
22. Goldenberg DM, DeLand FH, Bennett SJ, et al. Radioimmunodetection of prostatic cancer: in vivo use of radioactive antibodies against prostatic acid phosphatase for diagnosis and detection of prostatic cancer by nuclear imaging. *JAMA* 1983;250:630-635.
23. Carasquillo JA, Krohn KA, Beaumier P, et al. Diagnosis of and therapy for solid tumors with radiolabeled antibodies and immune fragments. *Cancer Treat Rep* 1984;68:317-323.
24. Goldenberg DM, Goldenberg H, Sharkey RM, et al. Clinical studies of cancer radioimmunodetection with carcinoembryonic antigen monoclonal antibody fragments labeled with <sup>125</sup>I or <sup>99m</sup>Tc. *Cancer Res* 1990;50:909s-921s.
25. Maguire RT, Schmelter RF, Pascucci VL, et al. Immunoscintigraphy of colorectal adenocarcinoma: results of site-specific radiolabeled B72.3 (<sup>111</sup>In-CYT-103). *Antibody Immunoconj Radiopharm* 1989;2:257-269.
26. Serafini AN, Vargas-Cuba R, Benedetto P, et al. Technetium-99m-labeled Fab' fragment of anti-CEA monoclonal antibody for radioimmunodetection of colorectal adenocarcinoma. *Antibody Immunoconj Radiopharm* 1991;4:561-568.
27. Sharkey RM, Goldenberg DM, Vagg R, et al. Phase I clinical evaluation of a new murine monoclonal antibody (Mu-9) against colon-specific antigen-p for targeting gastrointestinal carcinomas. *Cancer* 1994;73:864-877.
28. Stein R, Blumenthal R, Sharkey RM, Goldenberg DM. Comparative biodistribution and radioimmunotherapy of monoclonal antibodies RS7 and its F(ab')<sub>2</sub> in nude mice bearing human tumor xenografts. *Cancer* 1994;73:816-823.
29. Buist MR, Kenemans P, Holander W, et al. Kinetics and tissue distribution of the radiolabeled chimeric monoclonal antibody MOv18 IgG and F(ab')<sub>2</sub> fragments in ovarian carcinoma patients. *Cancer Res* 1993;53:5413-5418.
30. Murray JL, Rosenblum MG, Zhang HZ, et al. Comparative tumor localization of whole immunoglobulin G anticarcinoembryonic antigen monoclonal antibodies IMM-4 and IMM-4 F(ab')<sub>2</sub> in colorectal cancer patients. *Cancer* 1994;73:850-857.
31. Jain RK, Baxter LT. Mechanisms of heterogenous distribution of monoclonal antibodies and other macromolecules in tumors: significance of elevated interstitial pressure. *Cancer Res* 1988;48:7022-7032.
32. Jain RK. Determinants of tumor blood flow: a review. *Cancer Res* 1988;48:2641-2658.
33. van Osdol W, Fujimori K, Weinstein JN. An analysis of monoclonal antibody distribution in microscopic tumor nodules: consequences of a "binding site barrier." *Cancer Res* 1991;51:4776-4784.
34. Primus FJ, Newell KD, Blue A, Goldenberg DM. Immunological heterogeneity of carcinoembryonic antigen determinants on carcinoembryonic antigen distinguished by monoclonal antibodies. *Cancer Res* 1983;43:686-692.
35. Bosslet K, Steinsträsser A, Schwarz A, et al. Quantitative considerations supporting the irrelevance of circulating serum CEA for the immunoscintigraphic visualization of CEA expressing carcinomas. *Eur J Nucl Med* 1988;14:523-528.
36. Gasparini M, Buraggi GL, Regalia E, Maffioli L, Balzarini L, Gennari L. Comparison of radioimmunodetection with other imaging methods in evaluating local relapses of colorectal carcinoma. *Cancer* 1994;73:846-849.
37. Mariani G, Callegaro L, Mazzucca N, et al. Tissue distribution of radiolabelled anti-CEA monoclonal antibodies in man. *Protein Biol Fluids* 1984;32:483-486.
38. Baum RP, Hertel A, Lorenz M, Schwarz A, Encke A, Hör G. Technetium-99m-labeled anti-CEA monoclonal antibody for tumour immunoscintigraphy: first clinical results. *Nucl Med Commun* 1989;10:345-352.
39. Schwarz A, Steinsträsser A. A novel approach to Tc-99m-labeled monoclonal antibodies. *J Nucl Med* 1987;28:721.
40. Gasparini M, Ripamonti M, Seregini E, Regalia E, Buraggi GL. Tumor imaging of colo-rectal carcinoma with anti CEA monoclonal antibody. *Int J Cancer* 1988;(suppl) 2:81-84.
41. Riva P, Paganelli G, Cacciaguerra G, et al. Antibody guided tumor detection using <sup>131</sup>I-labeled F(ab')<sub>2</sub> fragments of an anti CEA MoAb. *Br J Cancer* 1985;52:649.
42. Riva P, Paganelli G, Callegaro L, et al. Immunoscintigraphy of adenocarcinomas by means of anti-CEA monoclonal antibody F023C5. *Nucl Med Commun* 1988;9:577-589.
43. Behr T, Becker W, Klein M, Stühler C, Scheele J, Wolf F. Immunoscintigraphy of colorectal cancer with <sup>99m</sup>Tc-labeled F(ab')<sub>2</sub> fragments of the anti-CEA MoAb F023C5. First clinical results. In: Bergmann, Sinzinger, eds. *Proceedings of the 21st Badgastein Symposium*. Wien: Birkhaeuser 1985:79-185.
44. Rhodes B, Zamora P, Newell K, Valdez F. Technetium-99m labeling of murine monoclonal antibody fragments. *J Nucl Med* 1986;27:685-693.
45. Behr T, Becker W, Hannappel E, Wolf F. Structural modifications of monoclonal antibodies following direct versus indirect labelling with <sup>99m</sup>Tc: does fragmentation really occur? *Nucl Med Commun* 1994;15:865-870.
46. Behr T, Becker W, Hannappel E, Goldenberg DM, Wolf F. Targeting of liver metastases of colorectal cancer with IgG, F(ab')<sub>2</sub>, and Fab' anti-CEA antibodies labeled with <sup>99m</sup>Tc: the role of metabolism and kinetics. *Cancer Res* 1995:in press.
47. Scatchard G. The attractions of proteins for small molecules and ions. *Ann NY Acad Sci* 1949;51:660-672.
48. Pimm MV, Rajput RS, Frier M, Gribben SJ. Anomalies in reduction-mediated technetium-99m labeling of monoclonal antibodies. *Eur J Nucl Med* 1991;18:973-976.
49. Mardirossian G, Wu C, Rusckowski M, Hnatowich DJ. The stability of Tc-99m directly labelled to an Fab' antibody via stannous ion and mercaptoethanol reduction. *Nucl Med Commun* 1992;13:503-512.
50. Hnatowich DJ, Mardirossian G, Rusckowski M, Fogarasi M, Virzi F, Winnard J. Directly and indirectly technetium-99m-labeled antibodies: a comparison of in vitro and animal in vivo properties. *J Nucl Med* 1993;34:109-119.
51. Gallup DG. Multicenter clinical trial of <sup>111</sup>In-CYT-103 in patients with ovarian cancer. In: Maguire RT, Van Nostrand D, eds. *Diagnosis of colorectal and ovarian carcinoma: application of immunoscintigraphic technology*. New York: Dekker; 1992:111-140.
52. Spiegelberg HL. Structure and function of Fc receptors for IgG on lymphocytes, monocytes and macrophages. *Adv Immunol* 1984;35:61.
53. Podoloff DA, Pott YZ, Curley SA, Krim EE, Bhadkamkar VA, Smith RE. Imaging of colorectal carcinoma with technetium-99m radiolabeled Fab' fragments. *Semin Nucl Med* 1993;23:89-98.
54. Schiessel R, Wunderlich M, Herbst F. Local recurrence of colorectal cancer: effect of early detection and aggressive surgery. *Br J Surg* 1986;73:342-344.
55. Adam IJ, Mohamdee MO, Martin IG, et al. Role of circumferential margin involvement in the local recurrence of rectal cancer. *Lancet* 1994;344:707-711.

56. Moertel CG, Fleming TR, Macdonald JS, Haller DG, Laurie JA, Tangen C. An evaluation of the carcinoembryonic antigen (CEA) test for monitoring patients with resected colon cancer. *JAMA* 1993;270:943-947.
57. Behr TM, Becker WS, Goldenberg DM, Wolf FG. Tumor targeting in liver metastases of colorectal cancer: a comparison of Tc-99m-labeled complete IgG<sub>1</sub> versus Fab' fragments. *J Nucl Med* 1994;35:56P.
58. Griffiths GL, Goldenberg DM, Diril H, Hansen HJ. Technetium-99m, rhenium-186 and rhenium-188 direct-labeled antibodies. *Cancer* 1994;73:761-768.
59. Griffiths GL, Goldenberg DM, Jones AL, Hansen HJ. Preparation of a pure <sup>99m</sup>Tc-F(ab')<sub>2</sub> radioimmunoconjugate by direct labeling methods. *Nucl Med Biol* 1994;21:649-655.